A Simple Subcortical Feeding Circuit Linking Interoceptive Inputs to Consummatory Behavior

Christin Kosse[1], Jessica Ivanov[1], Zachary Knight[2], Kyle Pellegrino[1] & Jeffrey Friedman[1*]

[1]Laboratory of Molecular Genetics, Howard Hughes Medical Institute, The Rockefeller University, 1230 York Avenue, New York, NY 10065, USA.

[2]Department of Physiology, University of California, San Francisco, San Francisco, CA 94158, USA

[*]Correspondence should be addressed to friedj@rockefeller.edu (J.M.F.)

Abstract

The brain processes an array of stimuli enabling the selection of an appropriate behavioural response but the underlying circuitry linking inputs to outputs is unknown. Here we delineate a subcortical circuit in which brain-derived neurotrophic factor (BDNF) expressing neurons in the ventromedial hypothalamus (VMH) directly connect interoceptive inputs to motor centers controlling food consumption. VMH^{BDNF} neuron inhibition increases food intake by gating motor sequences of feeding through projections to premotor areas in the brainstem. When food is unavailable, VMH^{BDNF} inhibition elicits consummatory behaviors directed at inanimate objects such as a wooden block. The activity of these neurons decreases prior to food consumption and increases when food is in proximity but not consumed. Their activity is higher in diet-induced obese animals dand also increased by leptin. VMH^{BDNF} neurons receive monosynaptic inputs from both agouti-related peptide (AgRP) and proopiomelanocortin (POMC) neurons in the arcuate nucleus (Arc) and AgRP inputs to these neurons increase food consumption. In addition, the orexigenic effect of AgRP neuron activation is blocked when VMH^{BDNF} neurons are also activated. These data identify a Arc^{AgRP}→VMH^{BDNF}→brainstem circuit that senses the energy state of an animal and elicits consummatory behaviors to control body weight.

Introduction

Understanding the principles of how innate behaviors are generated has long been the subject of intense theoretical and experimental inquiry but the precise neural mechanism underlying behavior selection are largely unknown (Lorenz, Tinbergen, Sherrington)[1–3]. Feeding is a typical innate behavior in which an array of sensory and interoceptive inputs are integrated to generate an adaptive behavioral response. However, because these many inputs typically change the probability of feeding, in contrast to a reflex, behavior initiation is context dependent and thus variable. While many brain areas and neuronal types have been identified that modulate feeding behavior, a complete neural circuit linking relevant sensory and interoceptive inputs to consummatory behaviors has not been identified. We thus sought to identify a neural pathway that directly connects interoceptive signaling to premotor centers that control consumption. Identifying the essential components of such a circuit would be informative in its own right and potentially provide a framework for investigating how top-down signals regulate innate behaviors[2]. Here we report the components of a simple circuit regulating feeding that directly

connects leptin signaling in the arcuate nucleus (Arc) to premotor areas in the brainstem that control food consumption.

The elements of this circuit emerged from studies aimed at identifying which population(s) of BDNF neurons regulate food intake and body weight. A role for BDNF neurons in feeding has been shown in studies of mice and humans carrying mutations in brain-derived neurotrophic factor (BDNF) or its receptor tyrosine kinase B (TrkB)[4–10]. Heterozygous mutations of BDNF or TrkB cause overconsumption and massive obesity in animals and humans. In addition, GWAS studies [11,12] have also suggested a role for BDNF in the development of obesity. However, because BDNF is widely expressed, the neural mechanism(s) responsible for the obesity and hyperphagia seen with defects in BDNF signalling are unknown. We initially set out to identify which BDNF neurons restrict overfeeding in animals fed a highly palatable diet. We found that a discrete subpopulation of BDNF neurons in the ventromedial hypothalamus (VMH), but not elsewhere, are activated by increased body weight after feeding mice a high fat diet (HFD). We thus set out to define the function of these neurons including the identification of their inputs and outputs. Here we report that VMH^{BDNF} act as a behavioral decision point for food consumption by directly linking neurons in the arcuate nucleus that receive interoceptive inputs to premotor sites in the brainstem that regulate mastication and other aspects of consummatory behavior.

Results

<u>BDNF expressing neurons in the VMH regulate food intake and body weight</u>

Mutations in BDNF or TrkB, its receptor, cause extreme obesity in mice and humans indicating that neurons that express these genes normally function to restrict food intake and weight gain. In order to elucidate the neural mechanism, we hypothesised that the key subpopulation of brain-derived neurotrophic factor (BDNF) expressing neurons would be activated when animals are placed on a HFD and gain body weight. This was investigated by identifying those BDNF neurons that show increased c-fos expression, an activity marker, in response to a HFD in BDNF-cre mice[13] mated to $Rosa26^{fsTRAP}$ mice expressing GFP in a cre dependent manner. Brain sections from HFD fed mice were then co-stained for both GFP (BDNF) and c-fos. This revealed extensive co-localization in the central and dorsomedial regions of the VMH (Fig.1a,b, 250.7±56.19 cells in HFD fed mice vs. 5.33±0.33 cells in sections from chow fed control mice) and nowhere else. Indeed, there was a nearly complete overlap between these markers in VMH with 98.32±0.69% of the neurons expressing c-fos also expressing BDNF (Fig. 1c). Further studies (Extended Data Fig.1d-f) revealed that 99% of the VMH^{BDNF} neurons colocalize with vesicular glutamate transporter 2 (Vglut2) and are thus glutamatergic. Furthermore, in situ hybridization for Sf1 and BDNF revealed that approximately half of the BDNF neurons in the dorsomedial VMH do not express SF1 (Extended Data Fig. 1a-f), confirming previous RNAseq[14] and immunohistology[15]studies showing that the BDNF expressing neurons are subpopulation and account for only ~ 10% of the neurons in this nucleus with small overlap with steroidogenic factor 1 (Sf1), a canonical marker for VMH that has been shown to be functionally distinct[16–18]. Thus, VMH^{BDNF} neurons represent a distinct subpopulation of VMH neurons that are specifically activated in animals fed a HFD. These

initial data thus suggested that VMH^{BDNF} neurons restrict food intake and weight gain. To directly test this possibility, we analysed the effect of selectively ablating VMH^{BDNF} neurons in mice fed chow and high fat diets.

VMH^{BDNF} neurons were ablated by injecting an adeno-associated virus (AAV) expressing a floxed diphtheria toxin A subunit (DtA) construct[19] into the VMH of BDNF cre mice (Fig. 1d-o). Chow fed mice with DtA ablation (Fig.1d-g) ate significantly more than controls (Fig.1m,) resulting in a significantly increased body weight (Fig.1l,) and body fat content (Fig.1g,). We next ablated VMH^{BDNF} neurons in animals fed a highly palatable diet (HPD) (Fig. 1h-k). Initially, mice with an ablation of VMH^{BDNF} neurons showed overfeeding like control mice (Fig. 1j and m,). However, while food intake in control animals fed a HPD decreased over time as weight increased, animals with VMH^{BDNF} neuron ablation continued to consume significantly more food (Fig.1j and n,). Body weight ultimately stabilized at a significantly higher level for DtA ablated mice (Fig.1i and l,). Mice with VMH^{BDNF} ablation also showed a significantly greater level of adiposity (Fig.1k,). These results show that VMH^{BDNF} neurons normally function to restrict overfeeding and obesity in animals fed chow and HPD diets.

<u>VMH^{BDNF} neurons bidirectionally control food intake</u>

To investigate whether control of food intake by VMH^{BDNF} neuron is dependent on neuronal activity, we next used optogenetics to either inhibit or activate these neurons. AAV strains encoding channelrhodopsin (ChR)[20] (Fig.2a,b) or Guillardia theta anion channelrhodopsin (GtACR)[21], (Fig.2e,f) were injected into the VMH of BDNF-cre mice and food intake was measured in response to light. To investigate whether VMH^{BDNF} neuron activity suppresses feeding even when mice are hungry, we fasted mice overnight and presented them with a chow pellet (Fig. 2c). Without light activation, control and ChR mice consumed similar amounts of food during the first 30 min. However, VMH^{BDNF} neuron stimulation at 2Hz completely inhibited food intake which returned to control levels when light stimulation ceased. Thus, VMH^{BDNF} neuron activation can entirely suppress the homeostatic, hunger-induced, drive to eat. To test whether VMH^{BDNF} neuron activity is also sufficient to suppress hedonic feeding, we presented sated chow fed mice with a highly palatable pellet of a high sugar and high fat content diet (Fig.2d). Control and ChR mice consumed similar amounts at baseline but optogenetic activation of VMH^{BDNF} neurons at 2Hz significantly decreased intake of the highly palatable pellets. We also found that in the period after light activation ceased, the mice in which VMH^{BDNF} neurons were activated now consumed even more than controls. These data show that VMH^{BDNF} neural activation significantly diminishes both homeostatic and hedonic feeding. We next tested the effect of VMH^{BDNF} neuron inhibition by measuring food intake in fed BDNF-cre animals expressing GtACR in the VMH. At baseline, control and GtACR mice consumed small but detectable amounts but during optogenetic inhibition, GtACR mice consumed significantly more food (Fig. 2g). To test whether inhibiting VMH^{BDNF} neuron activity would also increase the intake of HPD, we measured food intake after presenting mice with a HPD pellet. Initial intake prior to optogenetic inhibition was similar between control and GtACR mice while light induced neural inhibition again increased consumption (Fig.2h, Consistent with prior studies of animals fed a HFD [22,23], we observed (Fig.1j) that in control animals the initial hyperphagia of mice consuming a HPD intake diminished after 4 weeks as body weight approached a plateau at an ~20% higher level than that of chow fed mice. We also found increased levels of cFos

expression in BDNF neurons in DIO suggesting that because they are activated as weight is gained, they might act to restrict further weight gain. We thus tested the effect of inhibiting VMH^{BDNF} neural activity on acute consumption of a chow or HPD pellet in obese animals that had been fed a HPD for 4 weeks (Extended Data Fig.2a,b). Consistent with the studies of VMH^{BDNF} neuron inhibition in lean mice, the optogenetic inhibition of these neurons using GtACR in the obese mice increased consumption of chow and HPD pellets during the epochs of light exposure. (Extended Data Fig.2 c,d),). We also found that at baseline without optogenetic manipulation, the DIO mice acutely consumed less of a chow pellet than did lean chow fed animals (Extended Data Fig 2e). One potential explanation for the seemingly paradoxical finding that obese animals eat less chow than lean animals is that, as previously described, animals fed a highly palatable diet devalue chow [22,23]. However, we found that at baseline the DIO animals also consumed less of the HPD (Extended Data Fig 2f). We thus considered the possibility that this reduced consumption after obesity has developed might be a result of hyperactivity of VMH^{BDNF} neurons (see cFos data in Figure 1). If true, optogenetic inhibition of VMH^{BDNF} neurons should have a greater quantitative effect in DIO vs lean animals. Indeed, we found that optogenetic inhibition of VMH^{BDNF} neurons using GtACR resulted in a greater quantitative increase in the acute intake of HPD in DIO vs. lean animals (Extended Data Fig. 2g). We interpret this to mean that VMH^{BDNF} neurons are more active during the DIO state and thus act to restrict binge eating of a HPD. These studies show that VMH^{BDNF} neurons normally act to restrict intake of both chow and palatable food.

To further explore the mechanism by which VMH^{BDNF} neurons can control feeding, we tested whether VMH^{BDNF} neuron activity carries negative valence which would suggest a possible role in motivation. However, in an operant conditioning task, VMH^{BDNF} neuron activation failed to entrain a preference for self-inhibition (Extended Data Fig.3 a-c) and also failed to entrain a preference in a flavour conditioning assay (Extended Data Fig.3 d-f). These studies suggest that the effect of VMH^{BDNF} neurons on feeding is not mediated by a general effect on valence. An alternative possibility is that VMH^{BDNF} neurons regulate food consumption rather than food seeking. We tested this by analysing whether VMH^{BDNF} neuron inhibition influenced food approach vs. food consumption after optogenetic inhibition of VMH^{BDNF} neurons using two different paradigms: i. Constant photoinhibition for 5 min in an open loop (OL) system (Fig.2i,j) ii. inhibition in a closed loop (CL) system in which light was delivered only when the head of the mouse was within 3 cm of a chow pellet (Fig.2k,l). We found that the CL configuration led to a ~3 times greater food intake than did OL inhibition (Fig.2l). Consistent with this, the latency to approach the pellet was also increased 5-fold in the OL paradigm showing that VMH^{BDNF} neuron inhibition decreases the rate at which mice approach food (Fig.2m,). We also noted that OL VMH^{BDNF} neuron photoinhibition often triggered consummatory behaviour targeted at objects in immediate proximity to the mouse including the wall and bare floor of the cage. Thus, slowing the mouse down in its food approach and suggesting that these neurons might regulate motor behaviours associated with consumption. To characterise this further we studied the effect of VMH^{BDNF} neuron photoinhibition in the OL system in the presence of corn cob bedding (Fig.2n,o). We observed that animals would often chew the bedding during VMH^{BDNF} neuron photoinhibition and that the presence of bedding further decreased food intake compared to OL stimulation in a bare cage (Fig.2p). These data show that VMH^{BDNF} neuron inhibition drives feeding most effectively when food is in proximity to the animal and suggests the possibility that VMH^{BDNF} neurons regulate motor programs required for consumption independent of caloric value. To further evaluate this, we repeated the

CL study, but now provided the mice with a wooden block instead of a chow pellet (Fig. 2q-s). VMH^{BDNF} neuron inhibition in the CL led mice to spend ~9% of the trial duration engaged in biting the wooden block (Supplementary Video S1,). Taken together, these results suggest that inhibition of VMH^{BDNF} neuron activity increases food intake by triggering consumption of whatever objects are in proximity (such as a wood block or corn cob bedding) rather than by altering valence or food seeking. This finding is analogous to that seen after activation of central amygdala projections to the reticular formation, the motor pattern generator for killing bites[24]. Moreover, it raises the possibility that VMH^{BDNF} neurons represent a distal node, downstream of hedonic and homeostatic drives, in the neural circuit regulating feeding by controlling motor components of consumption such as biting and chewing. To test whether VMH^{BDNF} neuron inhibition would also elicit other types of biting such as aggressive biting, we put GTaCR expressing mice in an open field box with a female mouse (Extended Data Fig.3g,h) but failed to observe any biting attacks or aggression during optoinhibition. However, we noticed that inhibition reduced the amount of time mice spent interacting with the females drastically and still exhibited the same motor behaviors (i.e; biting) that in this case were directed at the wall and floor of the cage as previously observed with open loop inhibition (Fig. 2j).

<u>VMH^{BDNF} neural activity is inversely correlated with feeding and tuned to energy state</u>

The potent effect of VMH^{BDNF} neurons to reduce feeding suggested that the activity of these neurons might be decreased as they consume food and thus be permissive for feeding. We measured the in vivo activity of VMH^{BDNF} neurons using fiber photometery to monitor intracellular calcium levels when animals consumed or rejected food. BDNF-cre mice received injections of a cre dependent AAV encoding GCamp6s into the VMH (Fig. 3a) and calcium signals were measured during bouts of feeding. Time locked recordings showed a marked decrease in VMH^{BDNF} neuron activity coinciding with consumption of a chow pellet (Fig.3b, c, Supplementary Video S2,). This is consistent with the optogenetic results and suggests that VMH^{BDNF} neuron activity gates feeding behaviour and needs to be inhibited for feeding to commence. To test whether VMH^{BDNF} neuron activity would encode food palatability, we recorded during consumption of sucrose treat pellets which was associated with a similarly reduced activity (Fig. 3b,c,).

Having established that VMH^{BDNF} neuron activity is the same during consumption of chow and sucrose pellets, we investigated the effect of altered energy states by analysing neural activity under three sets of conditions, an overnight fast, chow feeding and feeding animals a HPD for 4 weeks (Fig 3d). Our previous data showing increased c-fos expression in VMH^{BDNF} neurons of HFD fed animals suggested that these neurons are activated in high energy states and act to decrease food intake. However, the baseline activity of these neurons in an empty home-cage showed no difference among these three conditions (Fig. 3,e,f). Rather, recordings of bouts of feeding show a ~65% higher level of activity of VMH^{BDNF} neurons in the DIO mice vs. chow fed animals (Fig. 3g,h). Similarly, the activity in VMH^{BDNF} neurons was ~23% lower in fasted vs. chow fed animals (Fig. 3 g-i,). We also noticed that when animals approached a chow pellet within a radius of 2 cm without subsequently consuming it, the calcium signal in VMH^{BDNF} neurons significantly increased (Fig. 3j-l, Supplementary Video S3,). In fasted mice there was a ~42% decrease in amplitude of the VMH^{BDNF} neuron when mice did not consume the pellet while in animals fed a HPD for 4 weeks there was an amplitude increase of ~80% when animals

approached but did not consume a pellet relative to the chow fed animals (Fig. 3l). In aggregate, these data show that VMH^{BDNF} neural activity is inversely correlated with food consumption and that activity responses are tuned to the animal's energy state.

VMH^{BDNF} neurons are downstream of Arc^{POMC} and Arc^{AgRP} neurons

Our finding that VMH^{BDNF} neural activity is altered by energy state raised the possibility that they might respond to the adipocyte derived hormone leptin[25,26]. This was tested by fiber photometry recordings after leptin vs. saline injections into fasted animals (Fig.4a-d). Leptin increased VMH^{BDNF} neural activity by ~75% when animals approached but did not consume a chow pellet or consumed a treat pellet (Extended Data Fig 4a-c,). To confirm that these neurons are necessary for leptin's effect on food intake we treated animals with leptin, ip 3mg/kg, after VMH^{BDNF} neural ablation with DtA (Extended Data Fig.3 d-f). The effect of leptin on food intake was significantly reduced in animals in which VMH^{BDNF} neurons were ablated. To test whether VMH^{BDNF} neurons can also respond to signals besides leptin, we crossed BDNF cre mice to leptin deficient ob/ob mice and injected DtA into the VMH (Extended Data Fig.3 g-i). ob/ob mice with VMH^{BDNF} ablation showed significantly increased food intake and became more obese. Because ob/ob mice lack leptin, these data indicate that VMH^{BDNF} neurons also sense other independent signals that normally act to restrict weight in ob/ob mice.

Prior anatomic[27] and single cell RNA sequencing studies[14] have indicated that VMH^{BDNF} neurons do not express leptin receptors, suggesting that leptin's effect on these neurons is indirect. Therefore, we next determined whether VMH^{BDNF} neurons receive inputs from the arcuate nucleus (Arc) (Fig. 4e), a key site of action for multiple interoceptive signals including leptin. The inputs to VMH^{BDNF} neurons were labelled by monosynaptic tracing with pseudotyped rabies[28,29]. We injected helper AAVs and G-deleted Rabies-mCherry viruses into the VMH of BDNF-cre mice and observed prominent inputs from Arc where leptin responsive POMC and AgRP neurons are located (Fig. 4f,g). We next performed multichannel FISH using probes for rabies, POMC and AgRP which revealed that a large proportion of Arc inputs are either POMC (42.28±7.95%) or AgRP (43.25±3.53%) neurons. In addition, many of the rabies labelled AgRP and POMC neurons also express the leptin receptor (Extended Data Fig.5a-e). Consistent with prior studies[30–32], in situ hybridization also revealed that 93±2.29% VMH^{BDNF} neurons co-expressed both neuropeptide Y receptor 5 (NPY5R) and melanocortin receptor 4 (MC4R), suggesting that VMH^{BDNF} neurons are a point of convergence for Arc^{POMC} and Arc^{AgRP} outputs (Extended Data Fig. 4f,g).

We next investigated whether the AgRP projections to the VMH can drive feeding similar to the effect of AgRP neuron somatic activation in the Arc[33]. A cre-dependent retrograde AAV encoding ChR was injected into the VMH of AgRP cre mice and optogenetic fibers were implanted above the VMH (Fig.4h). Optogenetic activation of the AgRP projections to the VMH increased food intake in chow fed mice (Fig.4i) but did not cause a decrease in food approach (Extended Data Fig. 5h-j). Moreover, closed loop activation targeted at a wood block did not elicit motor sequences of consummatory behavior (Fig.4j,k), suggesting that projection specific activation increases the likelihood of food intake but is not sufficient to trigger decisions for motor programs of food consumption. AgRP projections to the paraventricular hypothalamus (PVH) have also been reported to increase food intake via MC4R expressing neurons[34–36]. Retrograde tracing from VMH^{BDNF} neurons showed inputs from the PVH. In addition, in situ

hybridization of PVH neurons for MC4R after retrograde tracing revealed that VMH^{BDNF} neurons receive monosynaptic inputs from PVH^{MC4R} neurons (Extended Data Fig.5k,l).

assess whether VMH^{BDNF} neuron inhibition is generally necessary for the feeding and body weight effects of AgRP and POMC neurons, we simultaneously activated both Arc^{AgRP} and VMH^{BDNF} neurons by expressing NaChBac[37] in each or by activating Arc^{POMC} neurons using NaChBac and inhibiting VMH^{BDNF} neurons using tetanus toxin light chain (TelC)[38] (Fig.4 l-o). NaChBac is a bacterial sodium channel that leads to constitutive neural activation and TelC prevents vesicular release and thus silences neurons. AgRP cre mice were crossed to BDNF cre mice and an AAV expressing floxed NaChBac was stereotactically injected into the Arc and VMH (Fig.4l,m). Consistent with prior results[39], activation of Arc^{AgRP} neurons alone led to marked hyperphagia and obesity. Constitutive activation of VMH^{BDNF} neurons alone significantly reduced food intake and body weight. Finally simultaneous activation of both populations in double positive AgRP cre/BDNF cre mice fully recapitulated the effect seen with BDNF activation alone, showing significantly decreased food intake and weight. These data show that VMH^{BDNF} neurons are functionally downstream of Arc^{AgRP} neurons and a major output site.

The functional relationship between Arc^{POMC} and VMH^{BDNF} neurons was tested by crossing POMC dre mice to BDNF cre mice and injecting a dre dependent NaChBac into the Arc and a cre dependent TelC virus into the VMH (Fig.4p,q). Consistent with DtA ablation of VMH^{BDNF} neurons, BDNF cre mice expressing TelC alone showed significantly increased food intake and body weight (Fig.4r,s). Constitutive activation of Arc^{POMC} neurons led to a slight decrease of food intake and body weight which is consistent with prior studies[40]. Here again, the phenotype of the POMC dre/BDNF cre double positive mice recapitulated the phenotype of mice with constitutive inhibition of VMH^{BDNF} neurons alone. These data show that VMH^{BDNF} neurons are also functionally downstream of Arc^{POMC} neurons. Overall, this set of experiments shows that VMH^{BDNF} neurons are not just a simple relay but an integrator of interoceptive signals and outputs from neurons in the Arc and transition point to motor sequence control. Having established that VMH^{BDNF} neurons receive monosynaptic inputs from interoceptive neurons, we next investigated their functional outputs that are responsible for the motor sequences of consummatory behavior.

Projections from VMH^{BDNF} neurons to premotor areas in brainstem control consumption

We next mapped the projection sites of VMH^{BDNF} neurons to determine whether they projected to anatomic sites involved in the motor control of feeding. An AAV with a Cre dependent synaptophysin-Ruby gene was injected into the VMH of BDNF-cre mice (Fig.5a-c). Fluorescence imaging of neurons expressing Ruby revealed dense projections to the brainstem in the region of the mesencephalic nucleus (MesV) and reticular formation (RF), areas that have been shown to send anatomical and functional projections onto motor neurons of the jaw muscle[24,41–43]. To assess whether VMH^{BDNF} neurons project to premotor neurons regulating mastication, we simultaneously labelled VMH^{BDNF} neuronal projections with a cre dependent AAV expressing mGFP at the same time as premotor neurons with mCherry by injecting a retrograde AAV into the motor trigeminal nucleus (Mo5) that innervates the jaw muscles (Fig.5d-f). These data revealed that the projection sites of VMH^{BDNF} neurons are in close proximity to mCherry labelled premotor neurons projecting to the trigeminal nucleus (Fig.5f)

suggesting that VMH^{BDNF} neurons may regulate the activity of premotor neurons innervating the jaw. However, the targets of VMH^{BDNF} neurons are different from those downstream of Central Amygdala (CeA) neurons that control the killing bite of crickets during prey hunting[24]. This was shown using two AAV1 viruses encoding flp and cre as anterograde tracers[44]. Specifically, AAV1 flp was injected into the CeA and AAV1 cre injected into the VMH of cre reporter (GFP) mice crossed with flp reporter mice (tdTomato). This approach labeled CeA projection neurons in red and VMH projection neurons in green. The VMH projection neurons were localized primarily in MesV while the CeA projection neurons labelled a different, non-overlapping population of neurons in RF and MesV (Fig.5g-i). Our finding that the targets of the VMH^{BDNF} neurons are different from those from CeA is consistent with de Araujo's finding that the CeA-> RF circuit has no effect on food consumption.

We next assessed the function of this VMH^{BDNF} neuron→ brainstem projection by specifically activating nerve terminals in the region of the MesV/RF. Optical fibers were implanted above the RF in animals expressing ChR in VMH^{BDNF} neurons (Fig.5j-l). Similar to the effect of stimulating their soma, light stimulation of VMH^{BDNF} terminals in the reticular formation significantly suppressed chow intake in fasted mice provided with food and in chow fed mice given HPD. That the suppression of feeding by the brainstem projections is specific for motor outputs of biting and chewing was further shown by assessing the effect on food approach (Extended Data Fig.6a,b) and liquid diet consumption which were unaffected (Extended Data Fig 6c,d). We next investigated whether inhibition of the brainstem projections from VMH^{BDNF}neurons reduce food intake. A Cre dependent AAV encoding eOPN3, an inhibitory mosquito-derived rhodopsin, was injected into the VMH of BDNF cre mice and implants were placed above the projection sites in the brainstem (Fig.5m). Inhibition of the VMH^{BDNF} projections to brainstem increased food intake of both the chow and HPD diets (Fig.5n,o). In addition, inhibition of these projections also decreased food approach in OL inhibition (Fig.5p,q) and in the absence of food elicited the same motor sequences of biting and chewing of a wood block (Fig.5r,s) that were seen after inhibition of the soma. In aggregate, these data show that VMH^{BDNF} neurons directly transform interoceptive inputs from the arcuate nucleus into behavior decisions through projections to premotor sites that control consummatory motor actions (Extended data Fig.6e).

Discussion

A key function of the brain is to generate adaptive behaviors in response to an array of interoceptive and sensory inputs. A full understanding of how behaviors are controlled in higher organisms will thus require the elucidation of neural circuits linking sensory inputs to motor outputs. In this report we show that BDNF neurons in the VMH convey interoceptive inputs to motor outputs associated with feeding. These neurons comprise a small subpopulation of ~ 10% of the neurons in the VMH and integrate direct monosynaptic inputs from AgRP and POMC neurons in the Arc, two key interoceptive populations. In vivo imaging studies reveal that the activity of VMH^{BDNF} neurons is inversely correlated with feeding, tuned to energy state and modulated by leptin. Optogenetic activation of VMH^{BDNF} neurons prevents feeding while their inhibition increases food intake by driving motor sequences associated with feeding. These movements such as biting and grabbing of objects can be triggered even in the absence of food and directed at inedible objects such as a wood block. Finally, VMH^{BDNF} neurons project to

premotor sites in brainstem that regulate jaw and paw movements and activation of these projections also recapitulate the motor sequences of food consumption. In aggregate, these studies identify a simple circuit that directly links interoceptive inputs to motor outputs to control feeding.

In general, complex behaviors such as feeding, which are context dependent and thus variable, are considered as mechanistically distinct from a reflex in which a defined stimulus generally results in an invariant response. However, as suggested by Sherrington in 1906[2], the "transition from reflex action to volition(al) is not abrupt and sharp." Sherrington pointed out that reflexes are under volitional control noting that the cough reflex (and others) can be "checked, or released, or modified in its reaction with such variety and seeming independence of external stimuli by the existence of a spontaneous internal process expressed as will". This line of reasoning suggests the possibility that even among mammals feeding and other complex behaviors might be controlled in part by simple, reflex like circuits that are in turn modulated by descending inputs from higher centers as also suggested by Crick and Koch[45]. The possibility that relatively simple, subcortical circuits can regulated feeding is consistent with phylogenetic data from lower vertebrates that regulate feeding despite having only a very small or no cortex[46]. In addition, normal feeding is maintained in decorticate rats and rabbits so long as key diencephalic structures are intact[47,48]. The identification of an Arc→VMH^{BDNF}→brainstem circuit reported here supports Sherrington's hypothesis and now provides a framework for establishing a hierarchy among the many previously identified nodes that have been shown to control food intake[49,50]. However, the identification of this circuit does not preclude the possibility that other partially overlapping circuits may also regulate feeding by projecting onto the same or other premotor neurons. The delineation of this circuit may also provide the basis for an understanding of how specific instinctive behaviors are selected to the exclusion of other competing behaviors and thus has general implications for our understanding of action selection[1].

These data also show that VMH^{BDNF} neurons are a key functional output of AgRP neurons which play an essential role to drive food intake when an animal's energy state is low. While AgRP neuron activation by itself normally drives feeding, concurrent VMH^{BDNF} neuron activation entirely blocks this behavior. AgRP neurons act as interoceptive sensors of changes in energy state and drive all aspects of hunger[51,52] including both appetitive behaviors such as food seeking and consummatory behaviors. However, we find that AgRP inputs to VMH^{BDNF} neurons increase only the consummatory phase of feeding but not food approach, suggesting that other projection sites of these neurons regulate the motivational component. This is consistent with a hierarchical architecture for innate behaviors as proposed by Craig[53], Lorenz[3] and especially Tinbergen[1] in which appetitive and consummatory behaviors are separate and specific nodes regulating consumption are only "released" once food is in proximity and the appetitive phase is completed. Moreover, AgRP neuron projections to the VMH do not drive the consummatory motor sequences by themselves in the absence of food, suggesting that VMH^{BDNF} neurons may also receive an additional inhibitory signal to 'release' the motor programs for mastication. As suggested by Tinbergen, such inhibition could be sensory information derived from potential food sources that signal that food is in proximity. The possibility that VMH^{BDNF} neurons require

additional inputs besides AgRP neurons is analogous to Tinbergen's experiment in which honey bees only land on colorful artificial flowers when they are paired with appropriate odours[54].

The data also show that VMH^{BDNF} neurons are a critical node downstream of leptin signaling since leptin increases the gain of these neurons as shown using fiber photometry and DtA ablation of VMH^{BDNF} neurons decreases leptin's effect on food intake. Retrograde viral tracing from VMH^{BDNF} neurons identified the arcuate nucleus, the site of a circumventricular organ, as a neural input that conveys the leptin signal since VMH^{BDNF} neurons do not express leptin receptors themselves. Modulation of VMH^{BDNF} neural activity entirely blocks the effect of POMC or AgRP neural activation on feeding confirming that they are a key functional target of these neurons. This finding is in line with prior studies reporting the presence of POMC and AgRP fibers and terminals in the VMH[32,55]. Consistent with this, VMH^{BDNF} neurons co-express MC4R and NPY5R suggesting that they integrate both melanocortin and NPY feeding signals[32] and are a key integrator rather than a relay. Previous studies[56] have raised the possibility of a role for BDNF in the VMH downstream of MC4R signaling. Xu et al reported that BDNF injections can ameliorate the hyperphagic phenotype of A^Y mice and that BDNF expression in the VMH is regulated by melanocortin signaling. However, while we find MC4R expression in VMH^{BDNF} neurons, neither the functional effects of BDNF signaling in VMH on feeding nor the inputs or outputs of these neurons was evaluated. In addition to observing that the activity of VMH^{BDNF} neurons are modulated by leptin, we also find that they can also act independently of leptin to restrict further weight gain once obesity develops because ablating VMH^{BDNF} neurons increases weight even in ob/ob animals lacking leptin. It will now be important to understand which additional signals drive the increased activity of VMH^{BDNF} neurons in the obese state and whether these are mediated by melanocortins or other signaling pathways. A leptin independent effect is also consistent with a prior report showing that ob/ob mice receiving a six month infusion of leptin while on a high fat diet end up at a similar weight to wild type animals fed the same diet[57]. The fact that leptin levels were fixed in these ob/ob mice suggests that another signal(s) besides leptin was limiting the weight of this group. The data presented here are thus also consistent with the possibility both leptin dependent and leptin independent signals directly or indirectly activate VMH^{BDNF} neurons.

Consistent with data from mice with a BDNF knockout in the DMH and VMH, our results also suggest that ablation of VMH^{BDNF} neurons accounts for the massive obesity associated with lesions of the VMH in rodents[58,59] and humans[60,61].VMH^{BDNF} neurons appear to be distinct from Sf1 expressing neurons in the VMH and ablation of these neurons have very different effects. A postnatal knockout of Sf1, a canonical marker expressed in most VMH neurons, led only to a mild worsening of obesity in mice fed a high fat diet as a result of impaired thermogenesis with little or no change in food intake[62]. There is only a minimal effect in chow fed mice. We find only limited overlap between BDNF and Sf1 neurons which mark nearly all of the other neurons in this nucleus (~6% of SF1 neurons also express BDNF according to single cell RNA sequencing)[14]. Additonally, a prior report showed that an SF1 neuron specific deletion of BDNF does not affect feeding and body weight[16]. These data thus suggest that it is the subpopulation of BDNF neurons in VMH that accounts for the hyperphagia induced obesity that follows a VMH lesion. These data also suggest that VMH^{BDNF} neurons contribute significantly to the obesity associated with BDNF and TrkB mutations. Further support for this conclusion was provided in a recent study that found an interaction of BDNF and

astrocytes in the VMH that is essential for the suppression of obesity [63]. However, this does not exclude the possibility that other sites might also contribute to the overall effect of a BDNF or TrkB mutation. For example, while they do not regulate feeding, BDNF expressing neurons in the paraventricular nucleus have been shown regulate energy expenditure with effects on thermogenesis and adipose tissue innervation[64,65].

The data further suggest that VMH^{BDNF} neurons play a role in defining a set point for body weight once obesity develops. Large scale longitudinal studies have shown that body weight is remarkably stable over the course of a year (or longer) among not just lean but also obese individuals. For example, body weight typically returns to one's baseline even after periods associated with increased intake of calorie dense palatable meals such as Christmas and Golden Week[66]. This has suggested that weight and adipose tissue mass are under homeostatic control even among obese individuals or when highly palatable food is available. Similarly, when provided with highly palatable food, C57/Bl6 mice initially binge eat but as they approach a new, higher stable weight their food intake decreases. Our observation that VMH^{BDNF} neurons show c-fos activation and increased GCaMP transients in obese animals (Fig.1a and 4g-j suggests that these neurons are tuned to the energy state and prevent the development of an even more severe obese phenotype. Consistent with this ablating VMH^{BDNF} neurons increases body weight in both DIO and ob/ob mice. These data combined with the optogenetic manipulations suggest that these neurons act to maintain the set point when obesity develops.

Overall, these results show that VMH^{BDNF} neurons are a pivotal node that directly connects interoceptive inputs to motor actions. While mutations in BDNF and TrkB cause obesity in mice and humans[4–8], their relationship to other Mendelian forms of obesity was obscure. The circuit we identified connects leptin signaling, also a Mendelian form of obesity, to activation of a specific population of BDNF neurons and directly links them to neural pathways regulated by leptin as key components of the same neural circuit. Thus, VMH^{BDNF} neurons are a major outflow pathway of leptin signaling, though neural ablation studies indicate that they also integrate leptin independent signals serving as a multimodal integrator that controls body weight. The general importance of this Arc→VMH^{BDNF}→brainstem circuit is further amplified by our findings that, in contrast to other VMH populations, it accounts for the obesity associated with VMH lesions and establishes the set point for body weight in lean and obese animals.

In summary, these data show that VMH^{BDNF} neurons are a key element of a simple circuit that directly connect interoceptive inputs to motor outputs to regulate feeding and body weight. These results now provide a framework for studying the neural mechanisms by which higher centers may modulate feeding via actions on the Arc→VMH^{BDNF}→brainstem minimal circuit. This has important implications for the regulation of feeding and other complex motivational behaviors with basic and potential clinical implications.

References

1. Tinbergen, N. The hierarchical organization of nervous... *Symposia of the Society for Experimental Biology* **4**, 305–312 (1950).
2. Sherrington, C. S. *The integrative action of the nervous system*. xvi, 411 (Yale University Press, 1906). doi:10.1037/13798-000.
3. Lorenz, K. *The Foundations of Ethology*. (Springer Nature, 1981).
4. Gray, J. *et al.* Hyperphagia, severe obesity, impaired cognitive function, and hyperactivity associated with functional loss of one copy of the brain-derived neurotrophic factor (BDNF) gene. *Diabetes* **55**, 3366–3371 (2006).
5. Han, J. C. *et al.* Brain-derived neurotrophic factor and obesity in the WAGR syndrome. *N Engl J Med* **359**, 918–927 (2008).
6. Kernie, S. G., Liebl, D. J. & Parada, L. F. BDNF regulates eating behavior and locomotor activity in mice. *EMBO J.* **19**, 1290–1300 (2000).
7. Lyons, W. E. *et al.* Brain-derived neurotrophic factor-deficient mice develop aggressiveness and hyperphagia in conjunction with brain serotonergic abnormalities. *PNAS* **96**, 15239–15244 (1999).
8. Rios, M. *et al.* Conditional Deletion Of Brain-Derived Neurotrophic Factor in the Postnatal Brain Leads to Obesity and Hyperactivity. *Molecular Endocrinology* **15**, 1748–1757 (2001).
9. Yeo, G. S. H. *et al.* A de novo mutation affecting human TrkB associated with severe obesity and developmental delay. *Nat Neurosci* **7**, 1187–1189 (2004).
10. Unger, T. J., Calderon, G. A., Bradley, L. C., Sena-Esteves, M. & Rios, M. Selective deletion of Bdnf in the ventromedial and dorsomedial hypothalamus of adult mice results in hyperphagic behavior and obesity. *J Neurosci* **27**, 14265–14274 (2007).
11. Speliotes, E. K. *et al.* Association analyses of 249,796 individuals reveal 18 new loci associated with body mass index. *Nat. Genet.* **42**, 937–948 (2010).

12. Thorleifsson, G. *et al.* Genome-wide association yields new sequence variants at seven loci that associate with measures of obesity. *Nature Genetics* **41**, 18–24 (2009).

13. Luo, F. *et al.* Whole-brain patterns of the presynaptic inputs and axonal projections of BDNF neurons in the paraventricular nucleus. *Journal of Genetics and Genomics* **46**, 31–40 (2019).

14. Chen, R., Wu, X., Jiang, L. & Zhang, Y. Single-Cell RNA-Seq Reveals Hypothalamic Cell Diversity. *Cell Rep* **18**, 3227–3241 (2017).

15. Tran, P. V. *et al.* Diminished hypothalamic bdnf expression and impaired VMH function are associated with reduced SF-1 gene dosage. *Journal of Comparative Neurology* **498**, 637–648 (2006).

16. Kamitakahara, A., Xu, B. & Simerly, R. Ventromedial hypothalamic expression of Bdnf is required to establish normal patterns of afferent GABAergic connectivity and responses to hypoglycemia. *Mol Metab* **5**, 91–101 (2015).

17. Kennedy, A. *et al.* Stimulus-specific hypothalamic encoding of a persistent defensive state. *Nature* **586**, 730–734 (2020).

18. Kunwar, P. S. *et al.* Ventromedial hypothalamic neurons control a defensive emotion state. *eLife* **4**, e06633 (2015).

19. Wu, Z., Autry, A. E., Bergan, J. F., Watabe-Uchida, M. & Dulac, C. G. Galanin neurons in the medial preoptic area govern parental behaviour. *Nature* **509**, 325–330 (2014).

20. Boyden, E. S., Zhang, F., Bamberg, E., Nagel, G. & Deisseroth, K. Millisecond-timescale, genetically targeted optical control of neural activity. *Nature Neuroscience* **8**, 1263–1268 (2005).

21. Mahn, M. *et al.* High-efficiency optogenetic silencing with soma-targeted anion-conducting channelrhodopsins. *Nature Communications* **9**, 4125 (2018).

22. Beutler, L. R. *et al.* Obesity causes selective and long-lasting desensitization of AgRP neurons to dietary fat. *eLife* **9**, e55909 (2020).

23. Mazzone, C. M. *et al.* High-fat food biases hypothalamic and mesolimbic expression of consummatory drives. *Nature Neuroscience* **23**, 1253–1266 (2020).

24. Han, W. *et al.* Integrated Control of Predatory Hunting by the Central Nucleus of the Amygdala. *Cell* **168**, 311-324.e18 (2017).

25. Zhang, Y. *et al.* Positional cloning of the mouse obese gene and its human homologue. *Nature* **372**, 425–432 (1994).

26. Campfield, L. A., Smith, F. J., Guisez, Y., Devos, R. & Burn, P. Recombinant mouse OB protein: evidence for a peripheral signal linking adiposity and central neural networks. *Science* **269**, 546–549 (1995).

27. Liao, G.-Y. *et al.* Dendritically targeted Bdnf mRNA is essential for energy balance and response to leptin. *Nat Med* **18**, 564–571 (2012).

28. Lavin, T. K., Jin, L., Lea, N. E. & Wickersham, I. R. Monosynaptic Tracing Success Depends Critically on Helper Virus Concentrations. *Frontiers in Synaptic Neuroscience* **12**, (2020).

29. Liu, K. *et al.* Lhx6-positive GABA-releasing neurons of the zona incerta promote sleep. *Nature* **548**, 582–587 (2017).

30. Chen, Y. *et al.* Sustained NPY signaling enables AgRP neurons to drive feeding. *eLife* **8**, e46348 (2019).

31. Huszar, D. *et al.* Targeted Disruption of the Melanocortin-4 Receptor Results in Obesity in Mice. *Cell* **88**, 131–141 (1997).

32. Xu, B. *et al.* Brain-derived neurotrophic factor regulates energy balance downstream of melanocortin-4 receptor. *Nat Neurosci* **6**, 736–742 (2003).

33. Aponte, Y., Atasoy, D. & Sternson, S. M. AGRP neurons are sufficient to orchestrate feeding behavior rapidly and without training. *Nat Neurosci* **14**, 351–355 (2011).

34. Shah, B. P. *et al.* MC4R-expressing glutamatergic neurons in the paraventricular hypothalamus regulate feeding and are synaptically connected to the parabrachial nucleus. *Proc Natl Acad Sci U S A* **111**, 13193–13198 (2014).

35. Li, C. *et al.* Defined Paraventricular Hypothalamic Populations Exhibit Differential Responses to Food Contingent on Caloric State. *Cell Metabolism* **29**, 681-694.e5 (2019).

36. Li, M. M. *et al.* The Paraventricular Hypothalamus Regulates Satiety and Prevents Obesity via Two Genetically Distinct Circuits. *Neuron* **102**, 653-667.e6 (2019).

37. Xue, M., Atallah, B. V. & Scanziani, M. Equalizing excitation–inhibition ratios across visual cortical neurons. *Nature* **511**, 596–600 (2014).

38. Pashkovski, S. L. *et al.* Structure and flexibility in cortical representations of odour space. *Nature* **583**, 253–258 (2020).

39. Krashes, M. J. *et al.* Rapid, reversible activation of AgRP neurons drives feeding behavior in mice. *J Clin Invest* **121**, 1424–1428 (2011).

40. Jiang, J., Morgan, D. A., Cui, H. & Rahmouni, K. Activation of hypothalamic AgRP and POMC neurons evokes disparate sympathetic and cardiovascular responses. *Am J Physiol Heart Circ Physiol* **319**, H1069–H1077 (2020).

41. Moriyama, Y. Rhythmical jaw movements and lateral ponto-medullary reticular neurons in rats. *Comp Biochem Physiol A Comp Physiol* **86**, 7–14 (1987).

42. Sotgiu, M. L. & Marini, G. Projections from lateral reticular nucleus neurons to trigeminal motor nucleus revealed by antidromic activation in rabbits. *Exp Neurol* **98**, 26–33 (1987).

43. Stanek, E., Cheng, S., Takatoh, J., Han, B.-X. & Wang, F. Monosynaptic premotor circuit tracing reveals neural substrates for oro-motor coordination. *eLife* **3**, e02511 (2014).

44. Zingg, B. *et al.* AAV-Mediated Anterograde Transsynaptic Tagging: Mapping Corticocollicular Input-Defined Neural Pathways for Defense Behaviors. *Neuron* **93**, 33–47 (2017).

45. Crick, F. & Koch, C. A framework for consciousness. *Nat Neurosci* **6**, 119–126 (2003).

46. Wainwright, P. C. The evolution of feeding motor patterns in vertebrates. *Current Opinion in Neurobiology* **12**, 691–695 (2002).

47. Dellow, P. G. & Lund, J. P. Evidence for central timing of rhythmical mastication. *J Physiol* **215**, 1–13 (1971).

48. Whishaw, I. Q., Schallert, T. & Kolb, B. An analysis of feeding and sensorimotor abilities of rats after decortication. *J Comp Physiol Psychol* **95**, 85–103 (1981).

49. Andermann, M. L. & Lowell, B. B. Toward a Wiring Diagram Understanding of Appetite Control. *Neuron* **95**, 757–778 (2017).

50. Sternson, S. M. & Eiselt, A.-K. Three Pillars for the Neural Control of Appetite. *Annu Rev Physiol* **79**, 401–423 (2017).

51. Dietrich, M. O., Zimmer, M. R., Bober, J. & Horvath, T. L. Hypothalamic Agrp Neurons Drive Stereotypic Behaviors beyond Feeding. *Cell* **160**, 1222–1232 (2015).

52. Betley, J. N. *et al.* Neurons for hunger and thirst transmit a negative-valence teaching signal. *Nature* **521**, 180–185 (2015).

53. Craig, W. Appetites and Aversions as Constituents of Instincts. *Proceedings of the National Academy of Sciences of the United States of America* **3**, 685–688 (1917).

54. Tinbergen, N. *The study of instinct*. xii, 237 (Clarendon Press/Oxford University Press, 1951).

55. Wang, D. *et al.* Whole-brain mapping of the direct inputs and axonal projections of POMC and AgRP neurons. *Front Neuroanat* **9**, 40 (2015).

56. Xu, B. *et al.* Brain-derived neurotrophic factor regulates energy balance downstream of melanocortin-4 receptor. *Nat Neurosci* **6**, 736–742 (2003).

57. Knight, Z. A., Hannan, K. S., Greenberg, M. L. & Friedman, J. M. Hyperleptinemia Is Required for the Development of Leptin Resistance. *PLOS ONE* **5**, e11376 (2010).

58. Hetherington, A. W. & Ranson, S. W. Hypothalamic lesions and adiposity in the rat. *Anat. Rec.* **78**, 149–172 (1940).

59. Hetherington, A. W. & Ranson, S. W. The Spontaneous Activity and Food Intake of Rats with Hypothalamic Lesions. *American Journal of Physiology -- Legacy Content* **136**, 609–617 (1942).

60. Ga, B. & Jr, G. T. Manifestations of hypothalamic obesity in man: a comprehensive investigation of eight patients and a reveiw of the literature. *Medicine (Baltimore)* **54**, 301–330 (1975).

61. Pinkney, J., Wilding, J., Williams, G. & MacFarlane, I. Hypothalamic obesity in humans: what do we know and what can be done? *Obesity Reviews* **3**, 27–34 (2002).

62. Kim, K. W. *et al.* Steroidogenic factor 1 directs programs regulating diet-induced thermogenesis and leptin action in the ventral medial hypothalamic nucleus. *Proc Natl Acad Sci U S A* **108**, 10673–10678 (2011).

63. Ameroso, D. *et al.* Astrocytic BDNF signaling within the ventromedial hypothalamus regulates energy homeostasis. *Nat Metab* **4**, 627–643 (2022).

64. Wang, P. *et al.* A leptin–BDNF pathway regulating sympathetic innervation of adipose tissue. *Nature* **583**, 839–844 (2020).

65. Wu, S.-W. & Xu, B. Rapid and lasting effects of activating BDNF-expressing PVH neurons on energy balance. *eNeuro* ENEURO.0009-22.2022 (2022) doi:10.1523/ENEURO.0009-22.2022.

66. Helander, E. E., Wansink, B. & Chieh, A. Weight Gain over the Holidays in Three Countries. *N Engl J Med* **375**, 1200–1202 (2016).

67. Chen, T.-W. *et al.* Ultrasensitive fluorescent proteins for imaging neuronal activity. *Nature* **499**, 295–300 (2013).

68. Lerner, T. N. *et al.* Intact-Brain Analyses Reveal Distinct Information Carried by SNc Dopamine Subcircuits. *Cell* **162**, 635–647 (2015).

Methods

Mice

All animal care and experimentation were ethically performed according to procedures approved by the Institutional Animal Care and Use Committee at the Rockefeller University. Male mice were single housed in a 12-h light/12-h dark cycle with ad libitum access to regular chow and water except in fasting and DIO studies where either a HFD with 45 kcal%fat (4.7kcal/g) or a HPD with 42 kcal%fat and high sucrose content (4.5kcal/g) (TD.88137 Envigo) were provided. We used male ob/ob (B6.Cg-Lep^{ob}/J; 000632, Jackson Laboratory; or bred in-house), Rosa26^{fsTRAP} (B6.129S4-Gt(ROSA)26Sor$^{tm1(CAG-EGFP/Rpl10a,-birA)Wtp}$/J; 022367, Jackson Laboratory), AgRP-cre (AgRP$^{tm1(cre)Lowl}$/J; 012899, Jackson Laboratory), Flp reporter mice (RCF-tdTomato, B6.Cg-Gt(ROSA)26Sortm65.2(CAG-tdTomato)Hze/J; 032864, Jackson Laboratory) crossed to cre reporter mice (Rosa26^{fsTRAP}). BDNF-IRES-Cre mice were provided by W. Shen (Shanghai Institute of Technology). POMC-dre were provided by J. Bruning (Max Planck Institute for Metabolism Research). All mouse lines are in a WT (C57BL/6J) background. For brain surgeries, male mice of at least 8 weeks of age were anesthetized with isoflurane and placed into a stereotaxic frame (David Kopf Instruments), a craniotomy was performed, and a borosilicate glass pipette was used to inject viral vectors. For VMH injections: three injections (each 50□nL) were made into each hemisphere (bregma: −1.36□mm, midline: ±0.35□mm, from brain surface: 5.70□mm, 5.60 and 5.50□mm). For injections into the Arc 50nl were injected into: bregma: −1.45□mm, midline: ±0.45□mm, from brain surface: 5.70□mm, 5.60 and 5.50□mm, For injections into Mo5 75nl were injected into: bregma: -5.20mm, midline:±1.5mm, from brain surface: 4.60 and 4.50mm.

Reagents

leptin was diluted in sterile saline (3mg/kg) and injected intraperitoneally. For photometry recording mice were overnight fasted and injected with either saline or leptin 2h before recordings. All mice received saline and leptin injections in alternating order. For acute food intake experiments, leptin or saline was injected 2h before onset of the dark period and all mice received saline and leptin injections in a cross-over design.

Viruses

Cre dependent neuronal ablation was performed by injection of AAV1-mCherry-flex-dtA (UNC Vector Core)[19]. To target expression of the calcium activity indicator GCaMP6s to VMH^{BDNF} neurons, we used an AAV vector carrying a double floxed GCaMP6s construct (AAV5-Syn-Flex-GCaMP6s-WPRE-SV40, Addgene) [67]. For optogenetic manipulations, a somatic targeting GtACR (AAV5-hSyn1-SIO-stGtACR1-FusionRed) [21] or ChR (AAV5-EF1a-double floxed-hChR2(H134R)-EYFP-WPRE-HGHpA) were used (both Addgene). For long-term silencing a cre dependent TelC AAV (AAV5-hSyn-FLEX-TeLC-P2A-dTomato, Addgene) was used and for long-term activation a cre dependent NaChBac (AAV-Syn-DIO-NaChBac-dTomato) and a Dre dependent NaChBac (AAV5-hSyn-roxSTOProx-NaChBac-dTomato, HHMI-Janelia Research Campus) were used. For retrograde tracing a combination of two helper AAVs (AAV1-TREtight-mTagBFP2-B19G and AAV1-syn-FLEX-splitTVA-EGFP-tTA, both Addgene) and

pseudotyped rabies (EnvA G-Deleted Rabies-mCherry, Salk Institute) were injected. For projection activation we used an AAV encoding eOPN3 (AAV-hSyn1-SIO-eOPN3-mScarlet-WPRE, Addgene)[21] and for labelling projections with ChR we used a retro-AAV (AAV-EF1a-double floxed-hChR2(H134R)-mCherry-WPRE-HGHpA). Anterograde labelling was done with AAV1 encoding cre (AAV-hSyn-Cre-WPRE-hGH, Addgene) and flp (AAV-EF1a-Flpo, Addgene).

Immunofluorescence:

C-Fos staining after DIO: BDNF-cre mice were crossed to Rosa26fsTRAP to express eGFP in a cre dependent manner in BDNF neurons. Mice were fed a HFD whilst littermate control mice were fed chow. After 16 weeks mice were transcardially perfused with 4% PFA and the brains were post-fixed for 1 day in 4% PFA. Brains were then placed in 30% Sucrose in PBS until precipitation and frozen and coated in O.C.T. for cryosectioning. Cryosections (50µm) were cut using a Leica cryostat (CM1950). Brain sections were washed in PBS with 0.1% Triton X-100 (PBST, pH 7.4) and blocked in 3% normal goat/donkey serum (Jackson ImmunoResearch Laboratories) and 2% BSA (Sigma) in PBST for 2 h. Slides were then incubated overnight at room temperature in primary antibody. After washing in PBST, sections were incubated in fluorescein-conjugated goat IgG. Primary antibodies used and their dilutions: rabbit anti-FOS (1:1,000; mAb 2250S, Cell Signaling), chicken anti-GFP (1:1,000, ab 13970, Abcam). Secondary antibodies conjugated with Alexa-594, and Alexa-488 were purchased from Invitrogen. Brain sections were mounted onto SuperFrost (Fisher Scientific 22-034- 980) slides and then visualized with an inverted Zeiss LSM 780 laser scanning confocal microscope with a ×10 or ×20 lens. Images were imported to Fiji for further analysis and to count cells. To quantify the number of stained cells, brain slides were imaged under a ×20 objective.

For anterograde tracing: Brains were processed as described above and tdtomato and GFP were amplified with rabbit anti-RFP (1:1000, 600-401-379, Rockland) and chicken anti-GFP (1:1,000, ab 13970, Abcam) as primary antibodies and secondary antibodies conjugated with Alexa-594, and Alexa-488 were purchased from Invitrogen.

In situ hybridization

Mice were briefly transcardially perfused with RNase-free PBS to remove blood. Brains were then quickly collected, frozen in OCT, and stored at −80 °C until sectioning by cryostat (15µm sections) and attached on Superfrost Plus Adhesion Slides (Thermo Fisher). RNAscope® Fluorescent Multiplex assay (Advanced Cell Diagnostics Bio) was then performed using the RNAscope system. Probes for the following mRNAs were used (all from ACDBio): mm-BDNF (cat no. 424821) and eGFP (cat no. 400281), VGlut2 (cat no. 319171), RabV (cat no. 456781), AgRP (cat no. 400711), POMC (cat no. 314081), MC4R (cat no. 319181-C2) and NPY5R (cat no. 589811), LepR (cat no. 402731). In brief, RNAscope was used as per the manufacturer's protocol. Briefly, a hydrophobic barrier was created using Immedge Hydrophobic Barrier Pen (Vector Laboratories). Pre-treatment was done by serial submersion of the slides in 1× PBS, 50% EtOH, 70% EtOH and twice 100% EtOH for 2 min each, at room temperature. Probe hybridization was achieved by incubation of 35 µl mRNA target probes for 2 h at 40 °C using a HyBez oven. The signal was amplified by subsequent incubation of Amp-1, Amp-2, Amp-3 and

Amp-4 one drop each for 30, 15, 30 and 15 min, respectively, at 40□°C using a HyBez oven. Each incubation step was followed by two 2-min washes using RNAscope washing buffer. Nucleic acids were stained using DAPI Fluoromount-G (SouthernBiotech) mounting medium before coverslipping. Slides were visualized with an inverted Zeiss LSM 780 laser scanning confocal microscope using a ×20 or ×40 lens. Images were imported to Fiji for further analysis.

Long term body weight and food intake measures

Single housed mice were measured weekly to assess body weight and food intake. Whole-body composition was measured using Nuclear Magnetic Resonance Relaxometry (EchoMRI) at the end of the 16 weeks period.

Optogenetics

After injection of AAVs encoding either ChR or GtACR, we bilaterally implanted 200µm fiber optic cannulas (Thorlabs) in BDNF-cre mice and control mice (cre negative littermates). For VMH targeting, implants were angled at 15° and placed at bregma: −1.36□mm, midline: ±1.85□mm, from brain surface: 5.25□mm, for brainstem targeting implants were angled at 15° and placed at bregma: −5.25□mm, midline: ±1.75□mm, from brain surface: 2.6□mm) and subsequently fixed by dental cement (C&B metabond). After a minimum of 3 weeks expression time, mice were handled and habituated to tethering with optical fibers. A constant 473 nm laser (OEM Lasers/OptoEngine) was used for optogenetic inhibition with GtACR and pulsed at 2Hz (5ms) for optoactivation with ChR. For inhibition with OPN, a 532nm laser at 10Hz was used.

Lasers were connected to bifurcated optical fibers (Thorlabs) with an output of ~ 2-5mW at the implant., for AgRP projection stimulation the laser power was reduced to 1-2mW. Food intake studies were done in home cage like arenas during the light phase without bedding unless otherwise stated.

For acute food intake experiments with optogenetic activation or inhibition, mice were habituated to the arena for 10min without food present. Then consumption of a single food pellet was measured every 30min for 5 repetitions with only the second repetition being paired with optogenetic activation or inhibition. For open loop and closed loop feeding experiments, a single chow pellet was fixed to the middle of a home cage style arena with fun-tak (Loctite). Food intake was assessed every 5min in 3 repetitions with only the second repetition being paired with optogenetic inhibition. Inhibition was either 5min constant laser (open loop) or triggered (closed loop) by real time video tracking (Noldus, Ethovision) whenever the head of the mouse was within a 3 cm radius of the pellet. For modification with bedding present, the same open loop setup was used but with corn cob bedding covering the floor. For wood block trials, the chow pellet was replaced by a wood block that was fixed with fun-tak. Time spent biting the wood block was manually assessed and quantified by scoring of video recordings.

Liquid diet experiments were done with 20µl Ensure Vanilla pipetted onto the bare floor of a cage in 3 repetitions without light activation, followed by 3 repetitions with light activation and 3 repetitions without light activation. For quantification purposes, experiments were video recorded and latencies from Ensure delivery to full consumption were scored and averaged over the 3 repetitions.

Operant conditioning was performed in a home cage style arena with two capacitive touch plates mounted on opposing sides. Both touch plates were connected to an Arduino to register numbers of touches and one randomly assigned side would trigger cessation of constant 2Hz laser (for ChR) for 3 seconds or activation of a constant laser for 3 sec (for GtACR). Trials lasted for 1h.
Conditioned Flavor preference assays were performed as previously described [52]. Briefly, mice were habituated overnight to orange and strawberry flavored sugar-free Juicy Gels (Hunt's). Initial preference was assessed in a 30 min session without any light application. The preferred flavor was then paired with light exposure for ChR mice or the less preferred flavor paired with light exposure for GtACR mice. Conditioning was repeated daily for 3 days and consisted of one light exposure session where after 5 min light exposure started and lasted for 25min whilst the paired gel was presented and a 30min session with the non-paired gel without any light exposure. A 15 min test session where both gels were available was performed on the day after conditioning ended.

Fiber photometry

After an injection of AAV encoding cre dependent GCaMP6s into the VMH of male BDNF-cre mice, a unilateral 400µm fiber optic cannula was implanted as described for optogenetics. After a minimum of 4 weeks expression time, mice were habituated to tethering and a home cage style arena.
Data was collected with a Fiber Photometry system by Tucker-Davis Technologies (RZ5P, Synapse) and Doric components and recordings were synched to video recordings in Ethovision via TTL triggering. A 465nm and isosbestic 405nm LED (Doric) were reflected into a dual fluorescence Mini Cube (Doric) before entering the recording fiber that connects to the implant. Recording fibers were photobleached overnight before recordings to minimize autofluorescence. GCaMP6s fluorescence was collected as calcium dependent signal (525nm) and isosbestic control (430nm) with a femtowatt photoreceivers (Newport, 2151) and a lock-in amplifier via the RZ5P at a 1kHz sampling rate.
Mice were allowed to habituate for 30min at the start of each recording session before any items were introduced into the arena. Feeding bouts were manually assessed and scored from video recordings when mice were given single pellets of chow or 20mg sucrose treat pellets (Bio-Serv). Food interaction without consumption instances were defined as approach within a 2cm radius around a chow pellet without subsequent consumption. To measure the effect of different energy states, the same mice underwent the same standardized recording procedure at lean ad lib chow fed, overnight fasted injected with saline, overnight fasted injected with leptin and 4 weeks DIO. The order between lean, fasted saline, and fasted leptin were randomized to avoid any order effects.
Analysis was performed with a script written in Matlab based on a previously published method and code[68]. Bleaching and movement artefacts were removed by applying a polynomial least-square fit to the 405nm signal adjusting it to the 465nm trace (405_{fitted}) to then calculate the GCaMP signal as $\% \Delta F/F = (465_{signal}-405_{fitted})/405_{fitted}$. Traces were filtered with a moving average filter and down sampled by a factor 20. Three trials per mouse were averaged to derive data for peri-event plots and analysis of maximum and minimum signals.

Quantification and Statistic

Microscope images were analyzed and quantified in ImageJ/Fiji. Photometry recordings were processed and analyzed with MatLab (Mathworks). Statistical analysis was performed in GraphPad Prism. All tests are two-sided and results are displayed as mean±sem with statistical details in the figure legends including definition of n and significance. Significance was defined as $p<0.05$. Significance annotations are: $*p<0.05$, $**p<0.01$, $***p<0.001$, $****p<0.0001$. Mice were randomized into control or treatment groups. Control mice were age-matched littermate controls where possible. Graphs were produced using GraphPad Prism and Adobe illustrator with schematic illustrations prepared in BioRender.

Data availability

The data that support the findings of this study are available from the corresponding authors upon reasonable request. Requests for reagents should be directed to J.M.F.

Code availability

No novel code has been generated for the analysis of the data sets in this manuscript.

Methods references

53. Chen, T.-W. *et al.* Ultrasensitive fluorescent proteins for imaging neuronal activity. *Nature* **499**, 295–300 (2013).

54. Lerner, T. N. *et al.* Intact-Brain Analyses Reveal Distinct Information Carried by SNc Dopamine Subcircuits. *Cell* **162**, 635–647 (2015).

Acknowledgements

We thank all members of the Friedman lab for discussions and comments on the project, especially Anoj Ilanges. K. Hedbacker for breeding ob/ob mice and Rockefeller BIRC for microscopy. We thank Dr Bruning (Max Planck Institute) for the provision of POMC Dre mice. This work was supported by the JPB Foundation. C. K. is supported by a fellowship from the Leon-Levy Foundation.

Author contributions

C.K designed and performed all experiments. J.F. and C.K wrote the manuscript. Z.K. designed and performed the experiments. J.I and K.P. assisted C.K with experiments assisted.

Supplementary information

Supplementary Video 1: Optogenetic inhibiting of VMH^{BDNF} neurons when a mouse is near a wood block.

Supplementary Video 2: Photometry recording of a mouse approaching and consuming a treat pellet.

Supplementary Video 3: Photometry recording of a mouse approaching and not consuming a chow pellet.

Data Availability

The datasets generated and analysed during the current study are available from the corresponding author on reasonable request.

Code Availability

The code generated during the current study are available from the corresponding author on reasonable request.

Figure 1

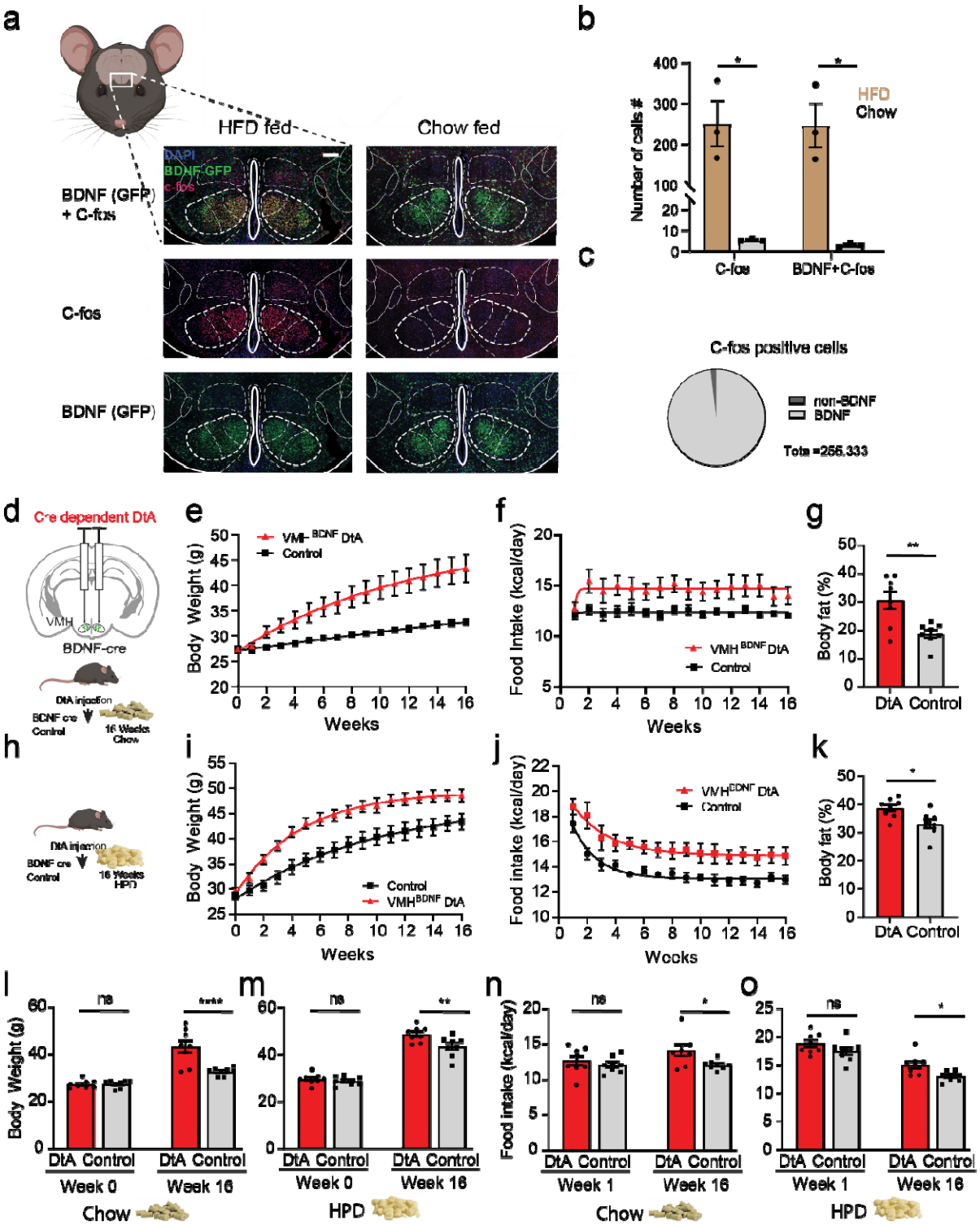
a
HFD fed
Chow fed
DAPI
BDNF-GFP
c-fos
BDNF (GFP) + C-fos
C-fos
BDNF (GFP)
b
Number of cells #
HFD
Chow
C-fos
BDNF+C-fos
c
C-fos positive cells
non-BDNF
BDNF
Total =255,333
d
Cre dependent DtA
VMH
BDNF-cre
DtA injection
BDNF cre
Control
16 Weeks Chow
e
Body Weight (g)
VMH BDNF DtA
Control
Weeks
f
Food Intake (kcal/day)
VMH BDNF DtA
Control
Weeks
g
Body fat (%)
DtA
Control
h
DtA injection
BDNF cre
Control
16 Weeks HPD
i
Body Weight (g)
Control
VMH BDNF DtA
Weeks
j
Food intake (kcal/day)
VMH BDNF DtA
Control
Weeks
k
Body fat (%)
DtA
Control
l
Body Weight (g)
ns
DtA Control
Week 0
Week 16
Chow
m
ns
DtA Control
Week 0
Week 16
HPD
n
Food intake (kcal/day)
ns
DtA Control
Week 1
Week 16
Chow
o
ns
DtA Control
Week 1
Week 16
HPD

Figure 1 VMH^{BDNF} neurons suppress food intake and body weight.

a, Schematic of a coronal brain slice containing the VMH and representative example of a hypothalamus section with immunolabelling for c-fos (red) and BDNF-GFP (green) after 16 weeks of HFD. Scale bar represents 200µm. **b,** Quantification of the number of c-fos positive and BDNF-GFP cells in the VMH of 3 mice. **c,** Quantification of c-fos positive cell expressing BDNF-GFP. **d,** schematic of bilateral DtA injection and experimental timeline for mice fed chow ad lib. **e,** weekly time course of body weight and calorie intake **(f)** of chow fed DtA (n= 8 mice) and control mice (n= 8 mice). **g,** Comparison of % body fat between DtA and control. 30.59±3.07% for DtA vs 18.85±1.37% for control, P=0.006, Unpaired t test with Welch's correction **h,** experimental timeline for mice fed HPD ad lib. **i,** weekly time course of body weight and calorie intake (**j**) of HPD fed DtA (n= 8 mice) and control mice (n= 8 mice). **k,** Comparison of % body fat between DtA and control on HPD. 38.66±1.22% for DtA vs 32.95±1.55% for control, P=0.0125, Unpaired t-test with Welch's correction **l**, Body weight comparison between DtA and control mice before DtA ablation and 16 weeks post-surgery. For chow 43.28±2.79g for DtA vs 32.68±0.60g for controls, P <0.0001, Two-way RM ANOVA with Šídák's multiple comparisons test. and **m**, HPD fed mice: 48.65±1.21g for DtA vs 43.42±1.57g for control, P =0.0055, Two-way RM ANOVA with Šídák's multiple comparisons test**. n,** Comparison of average daily calorie intake between DtA and control mice 1- and 16-weeks post-surgery for chow: 12.04± 0.24kcal for DtA vs 14.14± 0.80kcal for control, P =0.0303, Two-way RM ANOVA with Šídák's multiple comparisons test and **o**, HPD fed (right) mice. week 1: 18.77±0.65kcal in DtA vs 17.45±0.68kcal in controls, P=0.2355, Two-way RM ANOVA with Šídák's multiple comparisons test week 16: 14.99± 0.65kcal for DtA vs 12.98± 0.32kcal for control, P =0.047, Two-way RM ANOVA with Šídák's multiple comparisons test

Figure 2

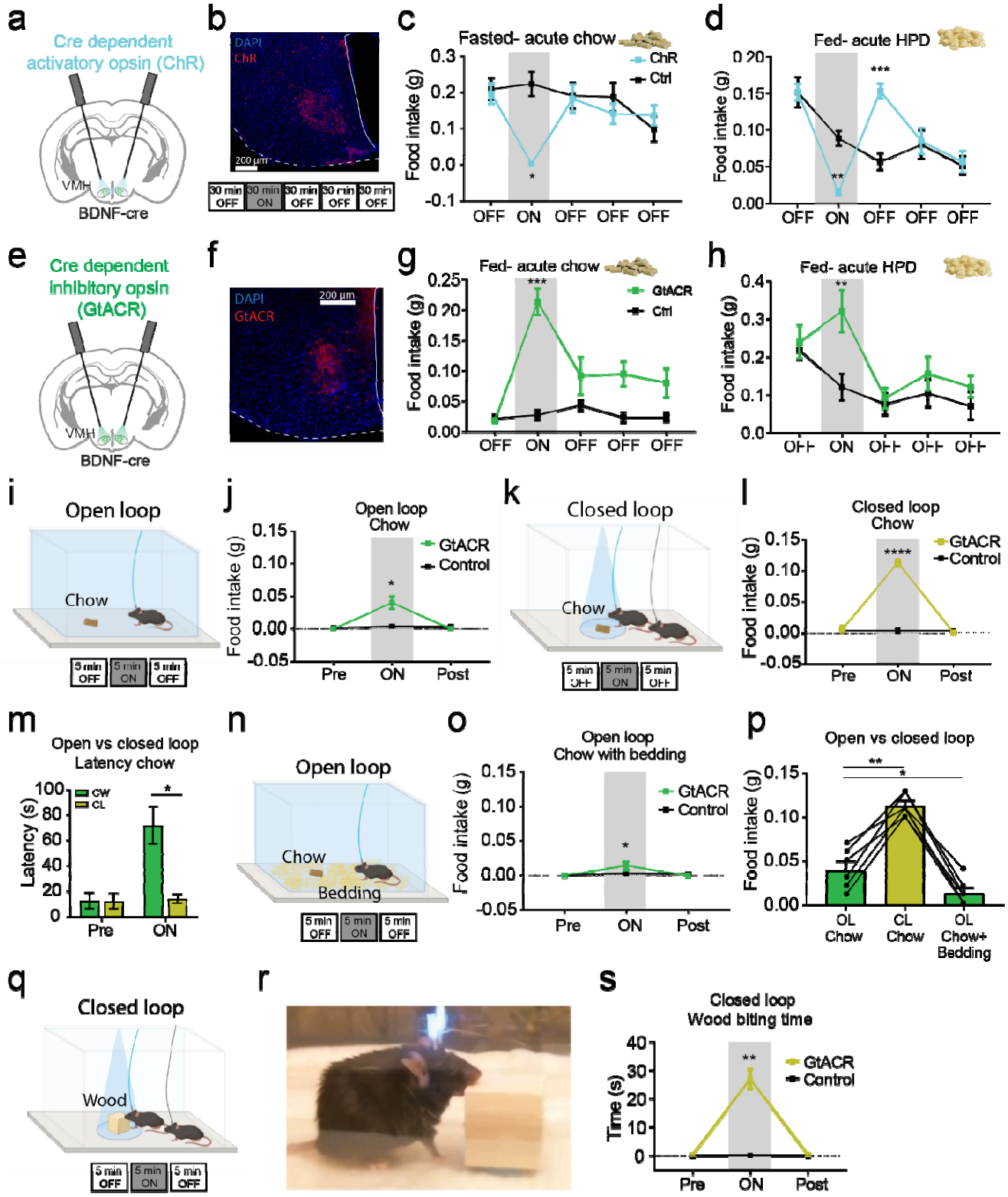
a
Cre dependent activatory opsin (ChR)
VMH
BDNF-cre
b
DAPI
ChR
200 µm
30 min OFF
30 min ON
30 min OFF
30 min OFF
30 min OFF
c
Fasted- acute chow
ChR
Ctrl
Food intake (g)
OFF ON OFF OFF OFF
d
Fed- acute HPD
Food intake (g)
OFF ON OFF OFF OFF
e
Cre dependent inhibitory opsin (GtACR)
VMH
BDNF-cre
f
DAPI
GtACR
200 µm
g
Fed- acute chow
GtACR
Ctrl
Food intake (g)
OFF ON OFF OFF OFF
h
Fed- acute HPD
Food intake (g)
OFF ON OFF OFF OFF
i
Open loop
Chow
5 min OFF
5 min ON
5 min OFF
j
Open loop
Chow
GtACR
Control
Food intake (g)
Pre ON Post
k
Closed loop
Chow
5 min OFF
5 min ON
5 min OFF
l
Closed loop
Chow
GtACR
Control
Food intake (g)
Pre ON Post
m
Open vs closed loop
Latency chow
OW
CL
Latency (s)
Pre ON
n
Open loop
Chow
Bedding
5 min OFF
5 min ON
5 min OFF
o
Open loop
Chow with bedding
GtACR
Control
Food intake (g)
Pre ON Post
p
Open vs closed loop
Food intake (g)
OL Chow
CL Chow
OL Chow+ Bedding
q
Closed loop
Wood
5 min OFF
5 min ON
5 min OFF
r
s
Closed loop
Wood biting time
GtACR
Control
Time (s)
Pre ON Post

Figure 2 VMH^{BDNF} neuron activity bidirectionally controls food consumption.

a, Schematic of ChR expression and optic fiber placement. **b,** Example of ChR expression with experimental timeline. **c**, Food intake of fasted ChR (n=6) and control mice (n=6) tested with acute chow (for ChR mice 0.002±0.002g vs 0.233±0.033g for controls, P=0.056, Two-way RM ANOVA with Šídák's multiple comparisons test) and **d,** fed mice with acute HPD. (For ChR mice 0.015±0.004g vs 0.088±0.010g for controls, P=0.0029, Two-way RM ANOVA with Šídák's multiple comparisons test) **e,** Schematic of GtACR expression and optic fiber placement. **f,** example of GtACR expression. **g**, Food intake of chow ad lib fed GtACR (n=6) and control mice (n=6) tested with acute chow and **h,** with acute HPD for ChR mice 0.153±0.010g vs 0.057±0.011g for controls, P= <0.0001, Two-way RM ANOVA with Šídák's multiple comparisons test). **i**, Schematic of open loop optogenetic inhibition and experimental timeline. **j,** Quantification of food intake of GtACR (n=6) and control mice (n=6). **k,** Schematic of closed loop optogenetic inhibition and experimental timeline. **l,** Quantification of food intake of GtACR (n=6) and control mice (n=6). **m**, Comparison of the latency to approach the chow pellet in open and closed inhibition for GtACR mice. 72.00±14.83s in OL vs 14.14±3.49s in CL P= 0.0139, Two-way RM ANOVA with Šídák's multiple comparisons test. **n,** Schematic of open loop optogenetic inhibition with bedding present and experimental timeline. **o,** Quantification of food intake of GtACR (n=6) and control mice (n=6). **p**, Comparison of food intake during optogenetic inhibition of 6 GtACR mice in the open loop, closed loop and open loop with bedding set up. ,0.04±0.010g for OL vs 0.113±0.006g for CL, P=0.0012, 0.04±0.010g for OL vs 0.013±0.006g for OL with bedding, P=0.018, Mixed-effects model (REML) with Dunnett’s multiple comparison **q**, Schematic of closed loop optogenetic inhibition with a wood block and experimental timeline. **r**, Example of consummatory biting behavior displayed by mice upon VMH^{BDNF} neuron inhibition. **s,** Quantification of % of time spent biting the wood block for GtACR (n=6) and control mice (n=6). 26.84±3.423s for GtACR mice vs 0.001±0.001s for controls, P=0.00166, Two-way RM ANOVA with Šídák's multiple comparisons test

Figure 3

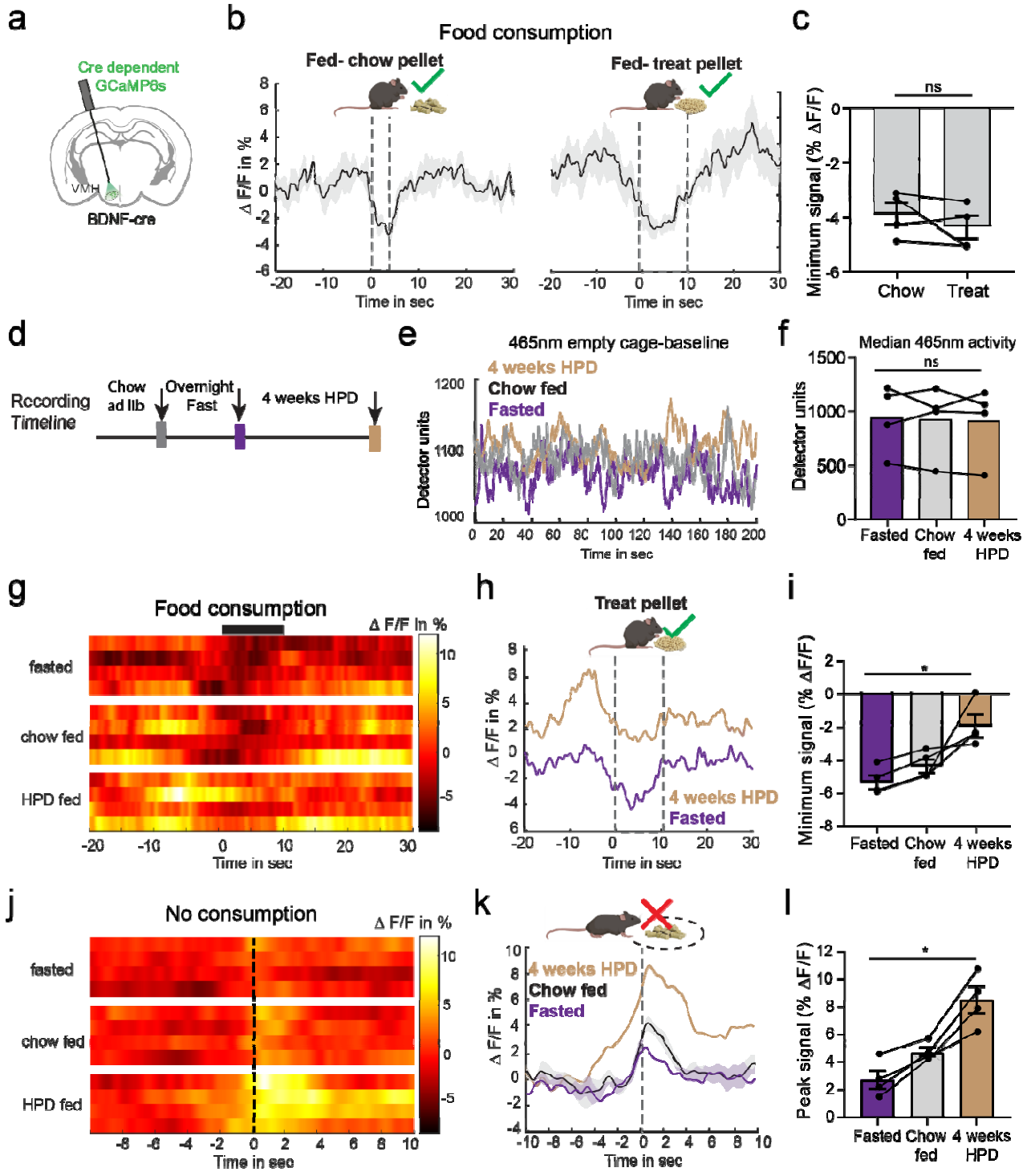
a
Cre dependent
GCaMP6s
VMH
BDNF-cre
b
Food consumption
Fed- chow pellet
Fed- treat pellet
Δ F/F in %
Time in sec
c
ns
Minimum signal (% ΔF/F)
Chow
Treat
d
Recording
Timeline
Chow
ad lib
Overnight
Fast
4 weeks HPD
e
465nm empty cage-baseline
4 weeks HPD
Chow fed
Fasted
Detector units
Time in sec
f
Median 465nm activity
ns
Detector units
Fasted
Chow fed
4 weeks HPD
g
Food consumption
Δ F/F in %
fasted
chow fed
HPD fed
Time in sec
h
Treat pellet
Δ F/F in %
4 weeks HPD
Fasted
Time in sec
i
*
Minimum signal (% ΔF/F)
Fasted
Chow fed
4 weeks HPD
j
No consumption
Δ F/F in %
fasted
chow fed
HPD fed
Time in sec
k
4 weeks HPD
Chow fed
Fasted
Δ F/F in %
Time in sec
l
*
Peak signal (% ΔF/F)
Fasted
Chow fed
4 weeks HPD

Figure 3 VMH^{BDNF} neuron activity is decreased during food consumption and tuned to energy state.

a, schematic of a coronal brain slice with GCaMP expression and fiber placement. **b**, average photometry trace ± sem (n=4 mice) aligned to a consumption bout of, left a chow pellet -3.869±0.402% for chow, P=0.0017, One sample t-test and right, a treat pellet in chow ad lib fed mice. **c**, comparison of the minimum signal between chow and treat pellet consumption (n=4 mice). -3.869±0.402% for chow vs -4.353±0.400% for sucrose treat, P=0.3438, Paired t-test **d**, recording timeline for energy state manipulations. **e**, 200s long example traces in detector units (not normalized) during empty cage exploration and comparison of the median thereof (**f**). **g**, heatmap of average photometry recordings per mouse (n=4 mice) aligned to a bout of treat pellet consumption. **h,** average overall photometry trace ± sem (n=4 mice) aligned to a bout of treat pellet consumption in fasted (purple) and 4 weeks HPD fed (beige) mice. **i**, comparison of the minimum signal during treat consumption. -4.353±0.400% in lean vs -5.339±0.419% in fasted vs -2.099±0.351% in DIO, P=0.0098, Mixed-effects model (REML) **j,** heatmap of average photometry recordings per mouse (n=4 mice) aligned to food approach without consumption. **k,** overall average overall photometry trace ± sem (n=4 mice) aligned food approach without consumption in fasted (purple) and 4 weeks HPD fed (beige) mice**. l,** comparison of the maximum signal.

Figure 4

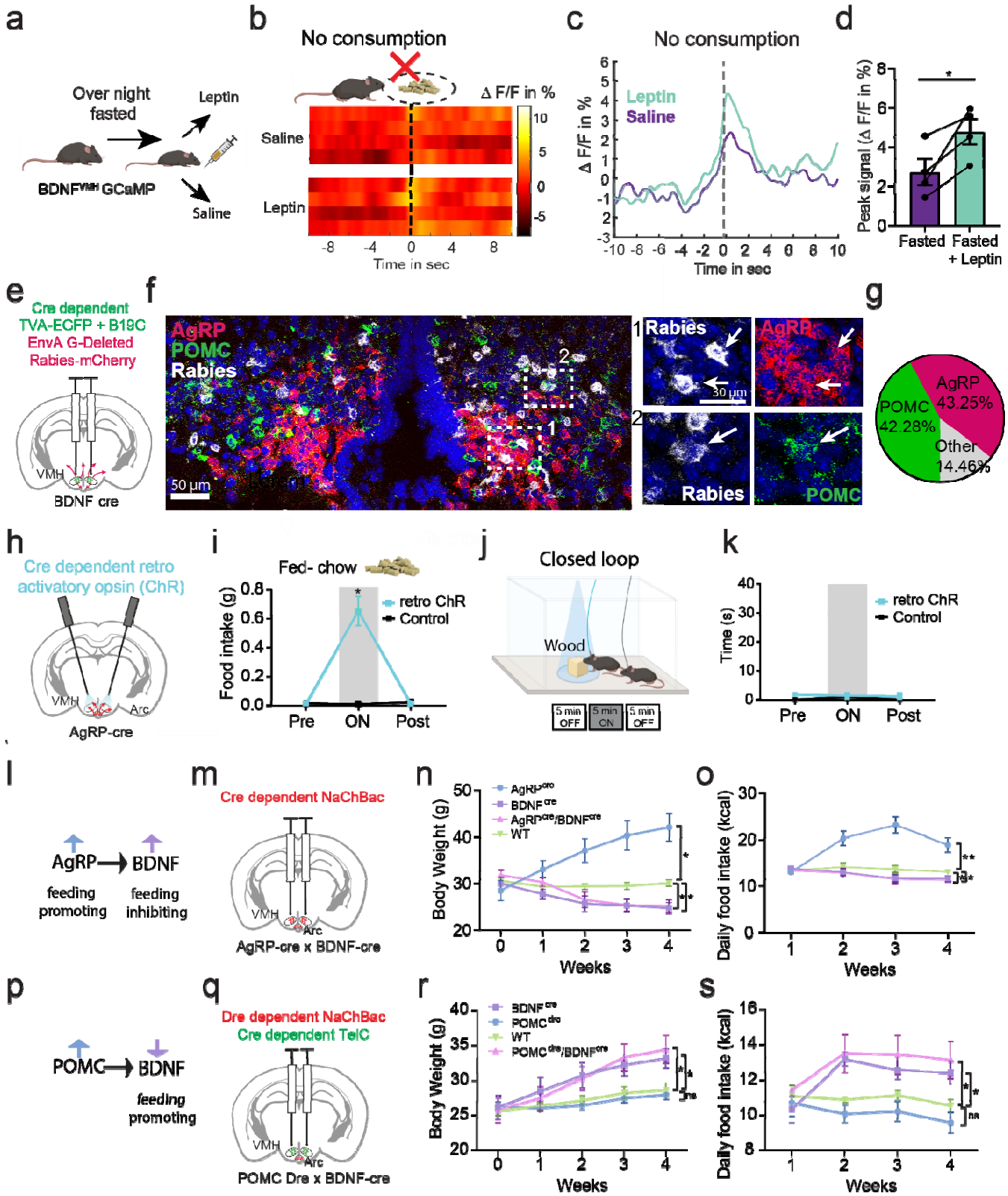
a
Over night fasted
Leptin
Saline
BDNF^VMH GCaMP
b
No consumption
Δ F/F in %
Saline
Leptin
Time in sec
c
No consumption
Leptin
Saline
Δ F/F in %
Time in sec
d
Peak signal (Δ F/F in %)
Fasted
Fasted + Leptin
e
Cre dependent
TVA-ECFP + B19C
EnvA G-Deleted
Rabies-mCherry
VMH
BDNF cre
f
AgRP
POMC
Rabies
50 µm
g
Rabies
AgRP
POMC
30 µm
AgRP 43.25%
POMC 42.28%
Other 14.46%
h
Cre dependent retro activatory opsin (ChR)
VMH
Arc
AgRP-cre
i
Fed- chow
retro ChR
Control
Food intake (g)
Pre
ON
Post
j
Closed loop
Wood
5 min OFF
5 min ON
5 min OFF
k
retro ChR
Control
Time (s)
Pre
ON
Post
l
AgRP
BDNF
feeding promoting
feeding inhibiting
m
Cre dependent NaChBac
VMH
Arc
AgRP-cre x BDNF-cre
n
Body Weight (g)
Weeks
o
Daily food intake (kcal)
Weeks
p
POMC
BDNF
feeding promoting
q
Dre dependent NaChBac
Cre dependent TelC
VMH
Arc
POMC Dre x BDNF-cre
r
Body Weight (g)
Weeks
s
Daily food intake (kcal)
Weeks

Figure 4 VMH^{BDNF} neurons are anatomically and functionally downstream of AgRP and POMC neurons

a, schematic of experimental design. **b,** heatmap of average photometry recordings per mouse and **c,** overall average photometry trace (±sem) (n=4 mice) aligned to food approach without consumption of mice injected with saline (purple) or leptin (green). **d,** comparison of the peak photometry signal: 2.718±0.675% saline injected vs in 4.778±0.657% leptin injected, P=0.0429, Paired t-test. **e,** Left, schematic of G-deleted pseudotyped rabies and helper AAV expression. **f**, representative example (n=3 mice) of a coronal Arc section with in situ hybridization for Rabies (white), AgRP (red) and POMC (green) and high magnification examples of the boxed area in (1) and (2). **g**, Quantification of average overlap of rabies labelled cells with AgRP and POMC in the Arc (n=3 mice). **h**, schematic of retrograde ChR expression in Arc and optic fiber placement in VMH. **i**, food intake of ad lib fed ChR (n=4) and control mice (n=4) tested with acute chow. **j**, schematic of closed loop optogenetic inhibition with a wood block and experimental timeline. **k**, quantification of % of time spent biting the wood block for ChR (n=4) and control mice (n=4). **l**, schematic of experimental hypothesis. m, schematic of bilateral expression of cre dependent NaChBac in Arc. n, weekly time course of body weight: AgRP cre 42.06 ±2.85g, BDNF cre 24.77±1.27g, AgRP cre/BDNF cre 25.21±1.32g, control mice 30.13±1.82g and calorie intake (**o**) of AgRP cre (n= 6 mice)16.86 ±2.06 kcal/day,BDNF cre (n=6mice) 11.53±0.76kcal/day, AgRP/BDNF cre (n=6mice) 11.37±0.55kcal and control mice (n= 7 mice) 13.14±1.29kcal/day after NaChBac injection. **p**, schematic of experimental hypothesis. q, schematic of bilateral expression of dre dependent NaChBac in Arc and cre dependent TelC in VMH. **r**, weekly time course of body weight:BDNF cre 33.75±1.40g, POMC dre 28.02±0.69g, POMC dre/BDNF cre 35.48±1.85g, control mice 28.78±2.40g and (**s**) calorie intake of POMC dre (n= 6 mice) 9.585±0.60kcal/day, BDNF cre (n=7mice) 12.42±0.48kcal/day, POMC dre/BDNF cre (n=7 mice) 13.22±0.80kcal/day and control mice (n= 7 mice) 10.56±0.98kcal/day after AAV injection.

Figure 5

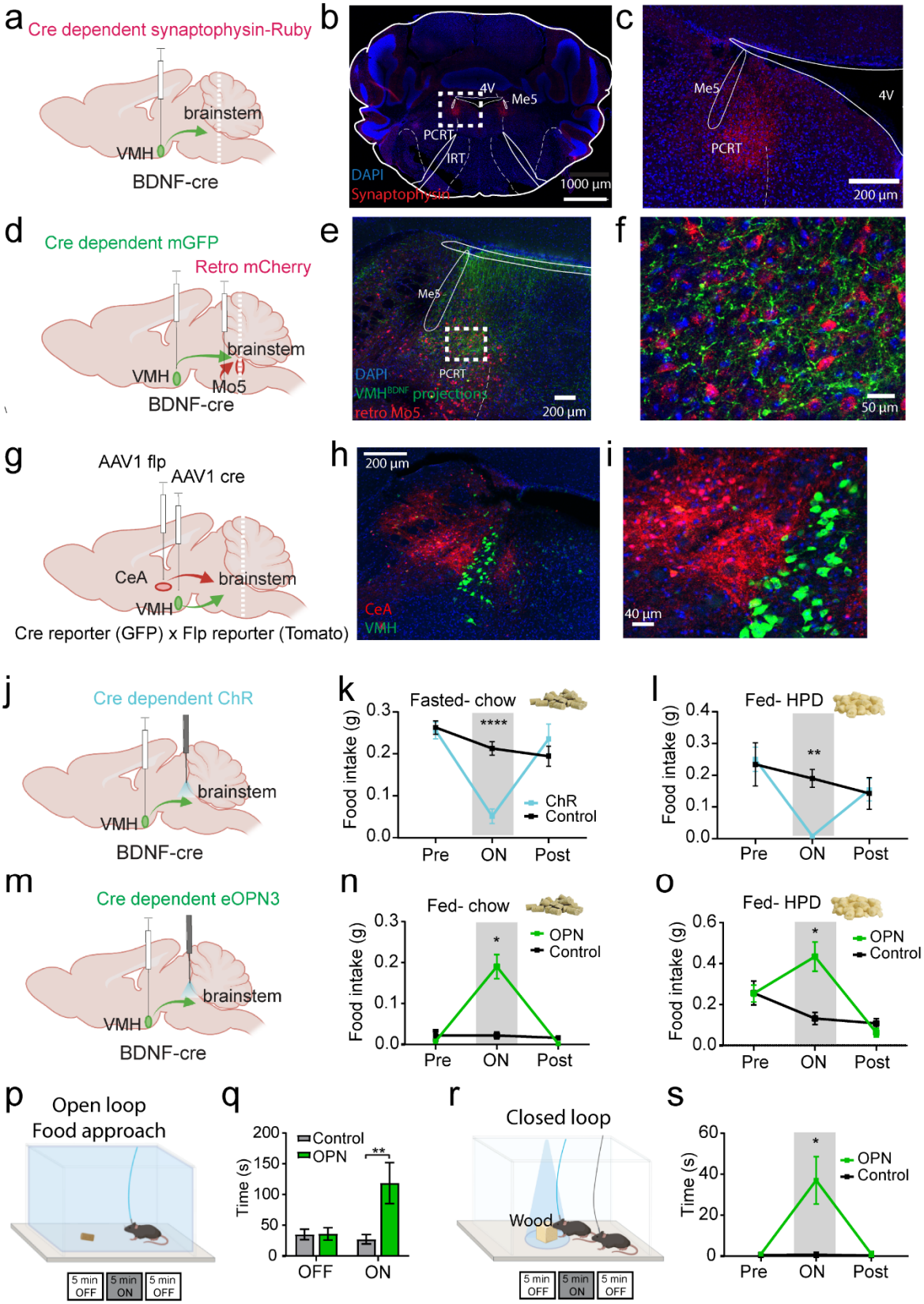
a
Cre dependent synaptophysin-Ruby
brainstem
VMH
BDNF-cre
b
4V
Me5
PCRT
IRT
DAPI
Synaptophysin
1000 µm
c
Me5
4V
PCRT
200 µm
d
Cre dependent mGFP
Retro mCherry
brainstem
VMH
Mo5
BDNF-cre
e
Me5
PCRT
DAPI
VMH^BDNF projections
retro Mo5
200 µm
f
50 µm
g
AAV1 flp
AAV1 cre
CeA
brainstem
VMH
Cre reporter (GFP) x Flp reporter (Tomato)
h
200 µm
CeA
VMH
i
40 µm
j
Cre dependent ChR
brainstem
VMH
BDNF-cre
k
Fasted- chow
Food intake (g)
0.3
0.2
0.1
0.0
****
ChR
Control
Pre
ON
Post
l
Fed- HPD
Food intake (g)
0.4
0.3
0.2
0.1
0.0
**
Pre
ON
Post
m
Cre dependent eOPN3
brainstem
VMH
BDNF-cre
n
Fed- chow
Food intake (g)
0.3
0.2
0.1
0.0
*
OPN
Control
Pre
ON
Post
o
Fed- HPD
Food intake (g)
0.6
0.4
0.2
0.0
*
OPN
Control
Pre
ON
Post
p
Open loop
Food approach
5 min OFF
5 min ON
5 min OFF
q
Control
OPN
Time (s)
200
150
100
50
0
**
OFF
ON
r
Closed loop
Wood
5 min OFF
5 min ON
5 min OFF
s
Time (s)
60
40
20
0
*
OPN
Control
Pre
ON
Post

Figure 5 VMH^{BDNF} neuron projections to the brainstem control food consumption.
a, schematic of a sagittal brain with synaptophysin-Ruby expression in the VMH and level of sectioning. **b,** representative (n=3 mice) coronal section of synaptophysin-Ruby (Red) expression and DAPI (blue) and **c,** a high magnification image of the boxed area. **d**, schematic of a sagittal brain with mGFP expression in the VMH and retro mCherry injected into Mo5 with dotted line indicating level of sectioning. **e**, representative (n=3 mice) coronal brain section of neurons projecting to Mo5 (Red), projections from VMH (Green) and DAPI (blue). **f,** high magnification image of the boxed area. **g,** schematic of virus injection into the CeA and VMH of Cre and Flp reporter expressing mice. **h**, representative example of n=3 mice of brainstem premotor areas (mesencephalic) and **i,** high magnification of AAV1 labelled neurons. **j**, schematic of a sagittal brain with ChR expression in the VMH and fiber placement above the brainstem. **k,** food intake of overnight fasted mice tested with acute chow (ChR: 0.05143±0.017g, Control: 0.2129±0.016g, P<0.0001, Two-way RM ANOVA with Šídák's multiple comparisons test) and **(l)** ad lib fed tested with HPD ChR (n=7) and control mice (n=7) (ChR: 0.008571±0.003g, Control: 0.1900±0.028g, P= 0.0019, Two-way RM ANOVA with Šídák's multiple comparisons test). **m,** schematic of a sagittal brain with eOPN3 expression in the VMH and fiber placement above the brainstem. **n,** food intake of ad lib fed mice tested with acute chow and **(l)** ad lib fed tested with HPD OPN (n=5) and control mice (n=5). **o**, schematic of open loop optogentic activation and experimental timeline for food approach**. p,** quantification of chow pellet approach in OPN mice (n=5) and control mice (n=5). **q**, schematic of closed loop optogenetic activation with a wood block and experimental timeline. **r**, quantification of % of time spent biting the wood block for OPN (n=5) and control mice (n=5). **s**, schematic of a proposed circuit for energy state driven food consumption behavior.